

## Cortical network fingerprints predict deep brain stimulation outcome in dystonia

**Gabriel Gonzalez-Escamilla, Muthuraman Muthuraman, Martin M. Reich, Nabin Koirala, Christian Riedel, Martin Glaser, Florian Lange, Günther Deuschl, Jens Volkmann, Sergiu Groppa**

### Angaben zur Veröffentlichung / Publication details:

Gonzalez-Escamilla, Gabriel, Muthuraman Muthuraman, Martin M. Reich, Nabin Koirala, Christian Riedel, Martin Glaser, Florian Lange, Günther Deuschl, Jens Volkmann, and Sergiu Groppa. 2019. "Cortical network fingerprints predict deep brain stimulation outcome in dystonia." *Movement Disorders* 34 (10): 1537–46.  
<https://doi.org/10.1002/mds.27808>.

## RESEARCH ARTICLE

# Cortical Network Fingerprints Predict Deep Brain Stimulation Outcome in Dystonia

Gabriel Gonzalez-Escamilla, PhD,<sup>1</sup> Muthuraman Muthuraman, PhD,<sup>1</sup> Martin M. Reich, MD, PhD,<sup>2</sup> Nabin Koirala, MSc,<sup>1</sup> Christian Riedel, MD,<sup>3</sup> Martin Glaser, MD, PhD,<sup>4</sup> Florian Lange, MD,<sup>2</sup> Günther Deuschl, MD, PhD,<sup>5</sup> Jens Volkmann, MD, PhD,<sup>2</sup> and Sergiu Groppa, MD, PhD<sup>1\*</sup>

<sup>1</sup>Department of Neurology, University Medical Center of the Johannes Gutenberg University Mainz, Mainz, Germany

<sup>2</sup>Department of Neurology, University Hospital Würzburg, Würzburg, Germany

<sup>3</sup>Department of Neuroradiology, UKSH, Christian-Albrechts-University Kiel, Kiel, Germany

<sup>4</sup>Department of Neurosurgery, University Medical Center of the Johannes Gutenberg University Mainz, Mainz, Germany

<sup>5</sup>Department of Neurology, UKSH, Christian-Albrechts-University Kiel, Kiel, Germany

**ABSTRACT: Background:** Deep brain stimulation (DBS) is an effective evidence-based therapy for dystonia. However, no unequivocal predictors of therapy responses exist. We investigated whether patients optimally responding to DBS present distinct brain network organization and structural patterns.

**Methods:** From a German multicenter cohort of 82 dystonia patients with segmental and generalized dystonia who received DBS implantation in the globus pallidus internus, we classified patients based on the clinical response 3 years after DBS. Patients were assigned to the superior-outcome group or moderate-outcome group, depending on whether they had above or below 70% motor improvement, respectively. Fifty-one patients met MRI-quality and treatment response requirements (mean age, 51.3 ± 13.2 years; 25 female) and were included in further analysis. From preoperative MRI we assessed cortical thickness and structural covariance, which were then fed into network analysis using graph theory. We designed a support vector machine to

classify subjects for the clinical response based on individual gray-matter fingerprints.

**Results:** The moderate-outcome group showed cortical atrophy mainly in the sensorimotor and visuomotor areas and disturbed network topology in these regions. The structural integrity of the cortical mantle explained about 45% of the DBS stimulation amplitude for optimal response in individual subjects. Classification analyses achieved up to 88% of accuracy using individual gray-matter atrophy patterns to predict DBS outcomes.

**Conclusions:** The analysis of cortical integrity, informed by group-level network properties, could be developed into independent predictors to identify dystonia patients who benefit from DBS. © 2019 The Authors. *Movement Disorders* published by Wiley Periodicals, Inc. on behalf of International Parkinson and Movement Disorder Society

**Key Words:** brain networks; clinical outcome; deep brain stimulation; dystonia

This is an open access article under the terms of the Creative Commons Attribution License, which permits use, distribution and reproduction in any medium, provided the original work is properly cited.

\*Correspondence to: Prof. Dr. Sergiu Groppa, Department of Neurology, Focus Program Translational Neuroscience (FTN), Rhine-Main Neuroscience Network (rnn), University Medical Center of the Johannes Gutenberg University Mainz, Langenbeckstrasse 1, 55131 Mainz, Germany; E-mail: segroppa@uni-mainz.de

**Relevant conflicts of interest/financial disclosures:** The authors report no disclosures or conflicts of interest concerning the research related to the article. No authors have received any funding from any institution, including personal relationships, interests, grants, employment, affiliations, patents, inventions, honoraria, consultancies, royalties, stock options/ownership, or expert testimony for the last 12 months.

**Funding agencies:** None.

**Received:** 14 January 2019; **Revised:** 2 July 2019; **Accepted:** 8 July 2019

Published online 21 August 2019 in Wiley Online Library (wileyonlinelibrary.com). DOI: 10.1002/mds.27808

Deep brain stimulation (DBS) is a well-established treatment for patients with medically intractable segmental and generalized dystonia, for which the globus pallidus internus (GPi-DBS) is an efficient target.<sup>1,2</sup> However, the degree of improvement varies among patients. Here, we postulated that structural brain network properties as derived from MRI may act as predictors in dystonia patients undergoing DBS. Furthermore, elucidating the neuroanatomical basis for network dysfunction in dystonia would have direct implications for surgical intervention<sup>3-5</sup> and is a critical first step toward developing personalized therapeutic solutions and effective neuromodulation paradigms. An individualized characterization of abnormal anatomical and physiological networks in each patient could lead to risk minimization for those patients who might be

susceptible to poor DBS outcomes because of specific disease fingerprints or irreversible secondary abnormalities in the brain circuits or periphery.

Brain circuit alterations have been attested to in patients with dystonia in several brain regions,<sup>6,7</sup> leading to the notion that the disease cannot arise from damage of a single structure, but rather from network dysfunction.<sup>8,9</sup> This network dysfunction leads to excessive movement that is normalized under DBS.<sup>10</sup> In addition, recent neuroimaging studies have suggested that the network of brain structures, including the basal ganglia and the cortex, present abnormal activation patterns both at rest and during voluntary movements in patients with dystonia.<sup>7,11</sup> Electrophysiological evaluations have further suggested that the loss of intracortical inhibition, increased cortical excitability in a cortico-subcortical network, and abnormal sensorimotor integration play a causal role in the pathophysiology of dystonia.<sup>10</sup> Importantly, GPi-DBS stimulation can attenuate this cortical hypersynchrony<sup>12,13</sup> and this effect has been shown to be dependent on the stimulation amplitude.<sup>14,15</sup> However, the extent to which these DBS-related effects rely on the structural integrity of the underlying cortical circuits remains unknown.

Here, we investigated how preoperative brain network properties relate to structural integrity fingerprints committing to the clinical outcome of GPi-DBS. For this, we reconstructed gray-matter cerebral networks using graph theory to quantify local and global structural patterns in patients with segmental and generalized dystonia.

Graph theory has become a relevant tool for exploring brain circuit abnormalities in neuropsychiatric disorders and for quantifying patterns of disease-related reorganization.<sup>16,17</sup> Small-world properties, which have been related to physiological brain functioning and reflect a clustered network with short paths, offer a basis for maintained network functionality and efficiency.<sup>18,19</sup> Despite the growing interest in DBS, much still remains unknown about the network-level impact of neuromodulatory effects. In this study, we sought to identify structural fingerprints that are related to network reorganization patterns and to predict the response and maintenance of benefit in a stable clinical state after 3 years of GPi-DBS using a novel computational approach consisting of graph theory and machine-learning techniques.

## Methods

### Standard Protocol Approvals, Registrations, and Patient Consents

This retrospective study was approved by the institutional review and ethics boards at each participating center and was carried out in accordance with the Declaration of Helsinki. All patients provided written informed consent.

### Study Participants and Data Acquisition

For a multicenter study including 82 primary dystonia patients who underwent GPi-DBS, 31 patients were not eligible because of poor MR image quality, namely, excessive image movement or ringing,<sup>20</sup> leaving a total of 51 patients (mean age,  $51.3 \pm 13.2$  years; 25 female) to be included in further analyses. This included a discovery cohort of patients treated at the University Clinic of Kiel ( $n = 36$ ; mean age  $\pm$  SD,  $50.1 \pm 12.1$  years; 16 female) and an independent test cohort from the University Clinic Würzburg ( $n = 15$ ; mean age  $\pm$  SD,  $54.2 \pm 9.3$  years; 9 female). None of the patients presented secondary dystonia. A more detailed description of these cohorts has been published previously.<sup>1,2</sup>

For the discovery dystonia cohort, patients underwent a T1-weighted magnetization-prepared rapid gradient-echo (MP-RAGE) MRI (repetition time [TR], 1140 milliseconds; echo time [TE], 4.4 milliseconds; inversion time [TI], 300 milliseconds; flip angle,  $8^\circ$ ; slice thickness, 1 mm; acquisition matrix,  $256 \times 256$ ; in-plane resolution, 1 mm) using a 1.5T Philips Achieva scanner with an 8-channel SENSE head coil. For the second cohort, again, high-resolution T1-weighted MP-RAGE images were acquired (TR, 1100 milliseconds; TE, 4.92 milliseconds; TI, 900 milliseconds; flip angle,  $20^\circ$ ; slice thickness, 1 mm; acquisition matrix,  $256 \times 256$ ; in-plane resolution, 1 mm) with a 3T Siemens TrioTim scanner, using a 32-channel SENSE head coil.

### GPi-DBS Electrode Implantation and Clinical Outcomes

Criteria for DBS indication comprised patient fail on anticholinergic treatment with at least 3 sessions of botulinum toxin treatment that resulted in unsatisfactory control of the dystonia. Patients with other neurologic or psychiatric disorders were further discarded from inclusion. All patients were implanted with bilateral electrodes (model 3387, Medtronic) in the posterior-ventral portion of the internal globus pallidus. The exact neurosurgical procedure has been described previously.<sup>1,21</sup> Standard stereotactic coordinates for anatomical targeting were individually adapted by direct visualization of the GPi on the MR images. Stimulation parameters including amplitude, frequency, and pulse width were adjusted for each individual patient. The effects of DBS on clinical outcomes were quantified as the improvement percentage in the movement scale of the Burke–Fahn–Marsden Dystonia Rating Scale for generalized dystonia<sup>2</sup> and the Toronto Western Spasmodic Torticollis Rating Scale for torticollis,<sup>1</sup> assessed before and 3 years after surgery. The improvement percentage at follow-up was further used to classify the patients as superior-outcome group (SOG) and moderate-outcome group (MOG). Stimulation adjustment and clinical evaluation were performed by clinicians who were blinded to the hypothesis and goals of this study.

Multiple independent reports have shown that in primary generalized and focal dystonias the average responses to GPi-DBS are up to of 60% to 70% of improvement in the respective motor scales after 3 years.<sup>22-24</sup> Accordingly, patients were classified based on their sustained clinical improvement into 2 demographically equivalent groups of MOG (lower than 70% in motor improvement,  $n = 26$ , 19 in the discovery cohort and 7 in the independent cohort) or SOG (motor improvement higher than 70%,  $n = 25$ ; 17 and 8 from each cohort respectively), see Table 1 for more details on the group distributions and demographics.

### Cortical Thickness Maps and Structural Covariance Network Measures

All T1 images were preprocessed using the automatic surface-based pipeline of FreeSurfer (v6.0, <http://surfer.nmr.mgh.harvard.edu>), which included: skull stripping, image affine registration, bias correction, and segmentation of gray- and white-matter tissue compartments, separation of brain hemispheres, and subcortical structures. At the end of the MRI preprocessing, 2 smooth surfaces were modeled per hemisphere, namely, the white (gray-to-white interface) and pial (gray-to-CSF interface) surfaces.<sup>25</sup> After reconstruction of the cortical surfaces, the distance from white to pial was used as a measure of cortical thickness at each vertex.

The cortical thicknesses of the 68 regions conforming the Desikan-Killiany atlas<sup>26</sup> was used to model the brain networks using graph theory.<sup>27</sup> First, for each group, the morphometric similarity, estimated as the Pearson product moment coefficient, was computed between each possible pair of regions across subjects. These pair-wise correlations were compiled into a covariance matrix with zero diagonal elements. Subsequently, the covariance matrix of each group was binarized with a network-derived threshold, in which an entry is 1 if the correlation weighting between a pair of regions is greater than a minimum density threshold, that is, the density at which all the regions are fully connected in the network of each group. This ensured that the networks in both groups had the same number of edges

and that the between-group differences reflected alterations in topological organization rather than differences in spurious correlations.<sup>28</sup> Consistent with previous studies,<sup>29</sup> the covariance matrices were thresholded at a range of network densities ( $n = 20$ ) from the minimum density in steps of 0.5% across a 10% degree range. This was done to allow for group differences testing and further construction of predictive models, while ensuring that such differences were not confounded by differing numbers of nodes and edges because of an absolute threshold at a single density. Related to graph theory based on covariance not yielding individual values of network measures, we first evaluated if the network behavior at the group level (using the metric values from all densities) was able to demask differences for the specific groups (MOG and SOG). Then, to go one step further, we took advantage of group-specific measures being created at different network densities ( $n = 20$ ) and extracted the values for each density to extend this model to evaluate, this time at the individual level, whether the structural integrity of the cortical regions showing network reorganization between the groups could be used as fingerprints of the DBS outcomes (see Fig. 1).

To evaluate network topology, the small-world index was calculated based on 2 key measures: the clustering coefficient ( $C$ , defined as the fraction of a node's neighbors that are also neighbors of each other); and the characteristic path length ( $P_L$ , the average minimum number of edges needed to cross from one node to all others).  $P_L$  and  $C$  were further normalized compared with a random network to avoid the influence of other topological characteristics, leading to the parameters "lambda" and "gamma," respectively. The network small-worldness, "sigma," was then calculated as the ratio of gamma to lambda ( $\sigma = \text{gamma}/\text{lambda}$ ).<sup>27</sup> Compared with a random graph, a small-world network is characterized as being highly clustered (clustering coefficient  $> 1$ , with higher values indicating large-scale network segregation) yet having a small characteristic path length ( $\sim 1$ , indicating large-scale network integration). Therefore,  $\sigma > 1$  describes optimal and efficient network topology.

In addition, the network's local efficiency ( $E_{\text{local}}$ , inverse of the average shortest path length; similar to  $C$ ,

**TABLE 1.** Group demographics

	Discovery cohort (1.5T MRI)			Validation cohort (3T MRI)		
	MOG ( $n = 17$ )	SOG ( $n = 19$ )	<i>P</i>	MOG ( $n = 8$ )	SOG ( $n = 7$ )	<i>P</i>
Generalized/cervical dystonia	9/8	10/9	0.98	1/7	5/2	<b>0.02</b>
Motor score (pre-DBS)	34.4 ± 15.9	27 ± 6.8	0.7	22.5 ± 1.7	24 ± 4.3	0.2
Motor score (follow-up)	21.2 ± 17.8	3 ± 1.3	<b>0.001</b>	16 ± 2.2	6 ± 1.5	<b>0.004</b>
% Motor improvement	40.4 ± 26.3	85 ± 2	<b>1.8 × 10<sup>-8</sup></b>	36.4 ± 9.6	80.2 ± 9.5	<b>0.001</b>
Disease duration	17.5 ± 11.9	12.4 ± 9.7	0.25	11.6 ± 10.4	12.35 ± 10.4	0.89
Female/male	7/10	9/10	0.7	5/3	4/3	0.8
Age ± SD	52.8 ± 11.4	47.7 ± 12.3	0.2	62.1 ± 9.3	45.1 ± 17.4	0.05

All clinical scores are presented as median ± standard error of the mean. MOG, moderate-outcome group; SOG, superior-outcome group. *P* values correspond to the comparison of SOG versus MOG in each cohort. The *t* test for continuous variables and chi-square for categorical variables (ie, dystonia type and sex).

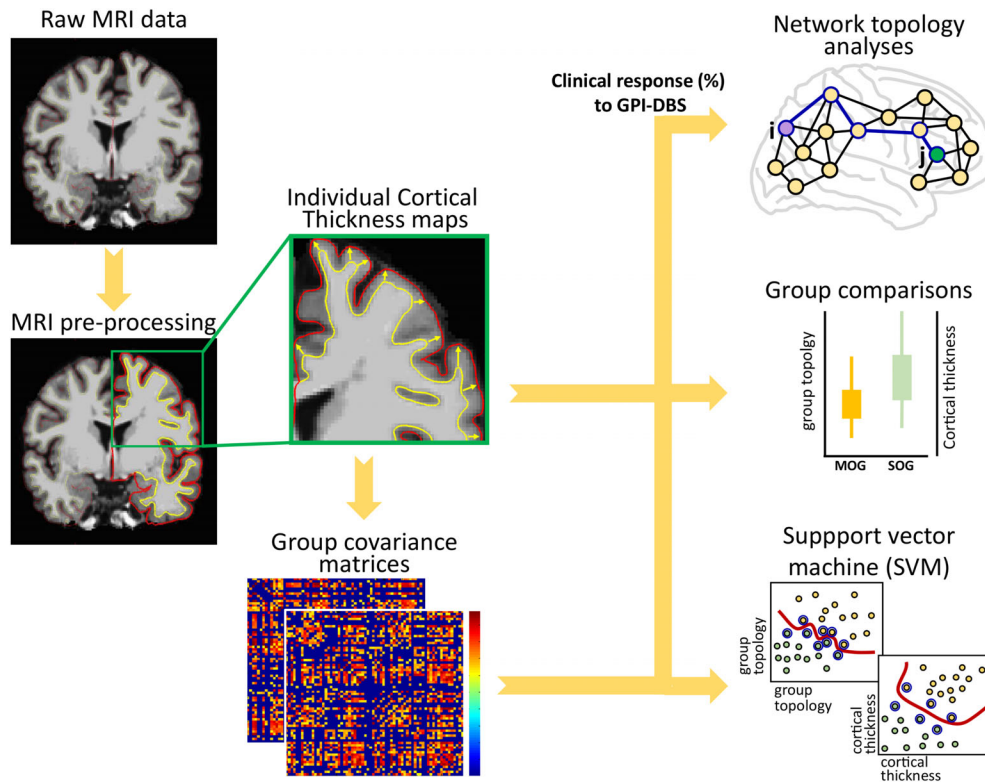


**FIG. 1.** General workflow for identifying putative image predictor markers of GPI-DBS clinical outcomes. From left to right: the MRI data were processed in FreeSurfer to obtain a regional estimation of cortical thickness (CT) and to construct the group covariance matrices. In each of the 2 cohorts, group-wise analyses between patients showing moderate outcome (MOG) and superior outcome (SOG) 3 years after GPI-DBS were then conducted for CT, subcortical volumes, and network topology (metrics: gamma, lambda, and sigma). For predicting the GPI-DBS responsiveness, as the network analyses do not straightforwardly allow deriving individual measures, we took advantage of the group-specific metrics being created at different network densities ( $n = 20$  for each group) and extracted the values for each density to create a group-level SVM to test the network parameters. To further bridge the connection between the individual structural markers and the network connectivity, the cortical thickness of the regions showing altered local connectivity and that in turn also showed decreased structure were used as individual “network-derived” features into the SVM. These 2 kinds of features (network metrics for all single densities and network-derived) were compared against a third model in which the volume of the subcortical structures showing group differences was used as features in the SVM. [Color figure can be viewed at [wileyonlinelibrary.com](http://wileyonlinelibrary.com)]

with larger values indicating a more segregated network), the nodal degree centrality (count of how many edges a single region has with the rest of the network) and nodal clustering (clustering coefficient of every single region) were used to evaluate the network topology from each region to its immediate neighbors. Detailed mathematical definitions of graph theory measures are found in the supplementary information. All network metrics and analyses were conducted in Matlab (R2013b, The MathWorks, Inc.) using the freely available brain connectivity toolbox.<sup>27</sup>

### GPI-DBI Outcome-Based Classification

Prior to further analyses, effects of age and sex were removed using the residuals of the GLM model as corrected estimates. First, the area under the curve (AUC) from receiver operating characteristic (ROC) curves was adopted to ensure the sensitivity of the network measures and cortical thickness of regions showing network differences to stratify the dystonia patients according to their GPI-DBS responsiveness.

Further, a nonprobabilistic binary support vector machine (SVM) classifier was used to test whether the DBS outcome can be predicted. Two different SVM models were conducted: (1) for the subcortical regions, the individual volume of each region that was significant in the group analysis was included in the first SVM; (2) after the regional network analyses, in which regions showing topological differences between MOG and SOG groups were identified, the individual cortical thickness values of these regions were included as features into the SVM. This latter variable is referred to as “network-selected cortical regions.” Briefly, the SVM algorithm looks for an optimally separating hyperplane that separates between the 2 data classes by maximizing the margin between the classes’ closest points. The points lying on the boundaries are called support vectors, and the middle of the margin is the optimal separating hyperplane (see Supplementary Information for further details). Here, we have used the polynomial function kernel for this projection because of its good performance.<sup>30</sup> We used a grid search (min = 1; max = 10) to find the few optimal input parameters, namely, C (capacity; 1 to 1000) and gamma (0.33). The SVM model

parameter selection was checked using 10-fold cross-validation. The support vectors from the input features were extracted and tested for the optimal parameter allowing computation of the correct classification ratio (CCR) and the model's precision and recall as indicators of success of prediction. To overcome the possibility that the classifier may be overfitted to the trained data and to have a more robust testing phase, the SVM classifier first constructed on the discovery cohort was then tested on an independent test data set (Würzburg cohort), hence, allowing direct comparison between the discovery and independent test cohorts while proving the model's generalizability.

### Statistical Analyses

Differences in cortical thickness between the 2 groups (SOG vs MOG) as well as associations between cortical thickness and stimulation parameters were statistically determined using the general linear model (GLM), with age and sex as nuisance variables using a threshold of  $P < 0.05$  corrected for multiple comparisons with 10,000 Monte Carlo  $Z$  simulations. Because of the bilateral implantation of the DBS electrodes, we assumed similarity in the morphometric integrity of the subcortical structures across left and right hemispheres. Hence, volumetric differences in the subcortical structures were studied without hemispheric differentiation. This allowed minimization of the problem of multiple comparisons. Nonetheless, results were corrected with a false discovery rate ( $P < 0.05$ ).

According to our aim of identifying structural fingerprints of GPi-DBS outcomes and under the hypothesis that the targeted regions may not be mainly responsible for the clinical outcomes, but the cortical regions associated with them, we address the dependence of the stimulation parameters from the structural integrity of the cortical mantle. For this we performed regression analyses between cortical thickness and stimulation intensity. Coefficients of determination ( $r^2$ ) are presented.

A GLM was used to test for between-group differences in each measure of network topology ( $C$ ,  $P_L$ ,  $\sigma$ ,  $E_{\text{local}}$ ) via a 2-sample  $t$  test. The statistical threshold for establishing significance was set at  $P < 0.05$ .

All statistical analyses between the 2 groups of interest (SOG vs MOG) were conducted independently in the 2 study cohorts (discovery and independent tests). Therefore, figures and tables summarize the results for each group in the discovery population and that were replicated/generalized aftermath to the second cohort.

### Data Availability

The data sets generated during and/or analyzed during the current study will be made available from the corresponding author on reasonable request.

## Results

### Demographics

When comparing the group ages, there was no significant difference between SOG and MOG in the discovery cohort ( $P = 0.2$ ,  $t = 1.3$ ) or the validated cohort ( $P = 0.05$ ,  $t = 2.2$ ). Similarly, no sex differences were found between SOG and MOG in the discovery (chi-square, 0.13;  $P = 0.7$ ) or independent test cohorts (chi-square, 0.04,  $P = 0.8$ ). Noteworthy, age and sex were still included as confounders in the statistical models to account for possible remaining effects. Further, no statistical differences in disease duration were observed between SOG and MOG in the discovery cohort ( $P = 0.3$ ,  $t = 1.17$ ) or the validated cohort ( $P = 0.9$ ,  $t = 0.14$ ).

### Preoperative Anatomical and Network Fingerprints

Correspondence of between-group differences in cortical thickness among populations (Fig. 2) was shown for cortical thinning in the superior, middle, and inferior (ventral motor area) frontal, paracentral, parietal (precuneus), and occipital (pericalcarine and lateral occipital) regions in MOG compared with SOG (discovery cohort,  $P = 1.5 \times 10^{-05}$ ,  $t = 4.8$ ; independent test cohort,  $P = 8.3 \times 10^{-05}$ ,  $t = 5.22$ ). Accordingly, in SOG patients the regression analyses showed a negative association between the mean cortical thickness of these areas and the DBS stimulation amplitude for the left ( $r^2 = 0.32$ ,  $P = 0.006$ ) and the right ( $r^2 = 0.2$ ,  $P = 0.03$ ) hemispheres, meaning that patients with more preserved cortical integrity require less intensity amplitudes to achieve the best clinical improvement. Such associations were only marginally seen in MOG (left:  $r^2 = 0.06$ ,  $P = 0.18$ ; right:  $r^2 = 0.17$ ,  $P = 0.06$ ). When using the average cortical thickness of both hemispheres (ie, assuming symmetry in the left/right pathology), we observed the same tendency: for SOG,  $r^2 = 0.27$  and  $P = 0.02$ ; and for MOG,  $r^2 = 0.13$  and  $P = 0.18$ . Subcortically, MOG also showed reduced volumes restricted to the caudate and putamen regions of the basal ganglia system (Table 2). No differences in the cerebellar grey matter were attested to.

For the discovery and the independent test cohorts, compared with SOG, MOG showed decreased small-worldness ( $\sigma$ ,  $t = 4.7$ ,  $P = 1.8 \times 10^{-5}$ ) and lambda ( $t = 3.82$ ,  $P = 0.0002$ ), and increased gamma ( $t = 3.81$ ,  $P = 0.0005$ ) and  $E_{\text{local}}$  ( $t = 1.6$ ,  $P = 0.05$ ). This indicates a less efficient network with fewer long-range connections (ie, more disconnected) for MOG and a preserved efficient topology in SOG (Fig. 3A). Consistent with the loss of long-range connections, the regional analyses revealed an increased degree of centrality in the central and frontoparietal regions in MOG (Fig. 3B). An increased clustering coefficient was also observed in the central and frontoparietal regions (Fig. 3C), evidencing a more divided network with higher density of local neighboring

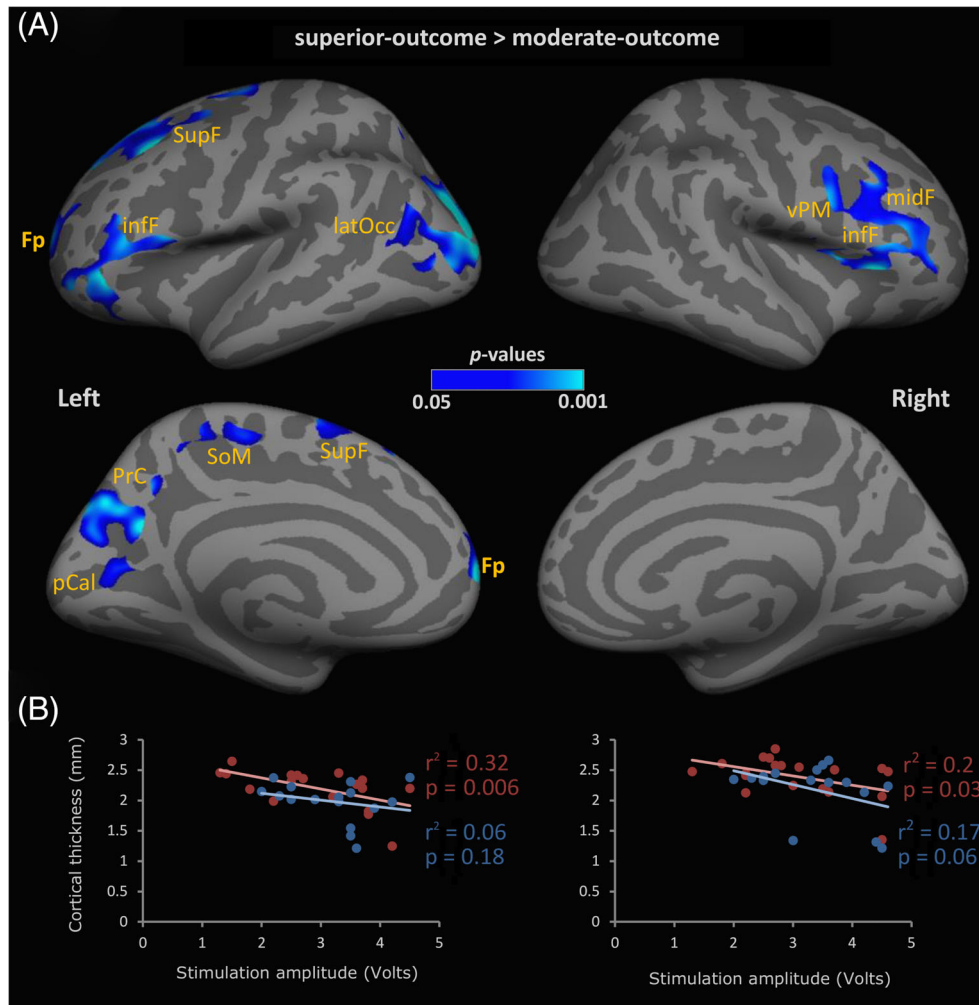


**FIG. 2.** Cortical thinning in the brain of the moderate-outcome group. (A) Overlap map depicting the regions where GPI-DBS moderate-outcome dystonia patients showed decreased cortical thickness compared with the superior-outcome group in both discovery and independent test cohorts. Top row, lateral hemisphere surfaces; bottom row, medial hemisphere surfaces. Fp, frontal pole; infF, inferior frontal; SupF, superior frontal; latOcc, lateral occipital; SoM, sensorimotor area (paracentral); PrC, precuneus; pCal, pericalcarine; vPM, ventral primary motor; midF, middle frontal. (B) Regression plots showing that patients with higher structural integrity require lower DBS stimulation amplitudes to achieve superior outcomes (red line). The same trend is observed for moderate-outcome (blue) groups. Nuisance variables: age and sex; *P* corrected for multiple comparisons using Monte Carlo Z simulations at *P* < 0.05. [Color figure can be viewed at [wileyonlinelibrary.com](http://wileyonlinelibrary.com)]

connectedness and low to no connection to distant regions (ie, segregation) in MOG. Given the high overlap between regions showing nodal network and cortical thickness differences between MOG and SOG, further SVM analyses were conducted to assess the ability of these network-identified regions to predict GPI-DBS responsiveness after 3 years.

### Predictors of GPI-DBS Responsiveness

Careful review of postoperative images showing the electrode location did not reveal any obvious deviation of the target in SOG and MOG patients.

When testing the ability of the network measures (across densities) to differentiate the patient groups for their clinical outcome (Fig. 3D), the highest AUC was for sigma (AUC, 0.86), followed by lambda (AUC, 0.7) and gamma (AUC, 0.73), with a mean accuracy (AUC, 0.73) for the

concatenated variable. For the individual measures the cortical regions with the highest power were left inferior-frontal (AUC, 0.82), left lateraloccipital (AUC, 0.85), and

**TABLE 2.** Group differences in GM subcortical volumes between GPI-DBS superior-outcome and moderate-outcome groups

GM nuclei	Discovery cohort		Validation cohort	
	<i>P</i>	T stat	<i>P</i>	T stat
Thalamus	0.21	0.83	0.24	0.7
Caudate	<b>0.015</b>	2.26	<b>0.017</b>	2.19
Putamen	<b>0.014</b>	2.31	0.062	1.57
Pallidum	0.44	0.14	0.2	0.84
Hippocampus	0.08	1.43	0.11	1.22

*P* values are corrected for multiple comparisons using false discovery rate.

left pericalcarine (AUC, 0.83), with the highest power for the combination of all (concatenated variable AUC, 0.88). For the individual subcortical volumes, both the combination of them and the caudate achieved a similar AUC (0.67) followed by the putamen (AUC, 0.62). This demonstrates that network topology and cortical atrophy have the most substantial influence on clinical outcome.

An SVM was then employed to test the ability of the individual regional morphometric integrity profiles, either of the cortical regions showing network reorganization or subcortical volumes showing group differences, to stratify the patients according to their clinical outcome (Fig. 3E). The analyses evidenced that group stratification through the cortical thickness measures of the network-selected regions achieved the maximum CCR (72.4%), followed by differentiation of subcortical volumes (CCR, 65.5%) in the discovery cohort. When testing the generalizability of the model in the independent test cohort, the accuracies were highly comparable for the subcortical volumes (CCR, 65.5%), whereas for the network-selected cortical regions, accuracy was increased about 10% (CCR, 80.6%).

## Discussion

Gray-matter network properties predict the clinical outcome to GPi-DBS in patients with dystonia. SOG presented brain circuits with a small-world topology. Patients with atrophy in a widespread network of association, sensorimotor, and visuomotor areas have disturbed network architecture and a worse long-term outcome. Furthermore, increased local connectivity was associated with worse clinical outcome.

In the current study the classification analyses allowed delimitation of superior-outcome versus moderate-outcome groups, both at the group and single subject levels. Network properties and regional gray-matter integrity information therefore represent putative correlates specific to brain behavior in patients with dystonia and are related to functional neuromodulation.<sup>10</sup> These shown network abnormalities are likely caused by reorganization of the parietal to frontal connections, with modified cortico-cortical or cortico-subcortical visuomotor and sensory information processing. These have been repeatedly related to abnormal motor control and generation of dystonic movements.<sup>31</sup> The regression analyses showed that in the SOG patients stimulation intensity is tightly associated with structural integrity of the cortex. Hence, the efficacy of DBS stimulation depends not only on the integrity of the stimulated region, but also on the connected regions. This hypothesis is also endorsed by the only marginal association found in MOG subjects, which together with the reduced cortical integrity in the frontal and posterior/motor regions, could limit their responsiveness to GPi-DBS. This

was further evidenced by the morphometric alterations in the basal ganglia and thalamus in MOG.

Alterations within the sensorimotor and associative circuits, involving central, frontal, and parietal cortices, have been reported, suggesting that dystonia may represent a disorder of large-scale networks as opposed to local pathology alone.<sup>6,8</sup> In support of this novel view, a loss of long-range connections was shown in MOG to DBS. As increased clustering coefficients indicate a fewer number of edges between distant regions (ie, long-range connections), and reduced path lengths indicate that the integrative properties of the network are diminished,<sup>18,28</sup> both findings point toward a more segregated (ie, divided) and less efficient network organization in MOG. In such segregated network, increased local efficiency evidences that when the long-range connections disappear, the majority of the remaining edges will be among neighboring regions (see Supplementary Fig. 1). Therefore, in MOG the regional increase in degree of centrality and clustering coefficient can be interpreted as increased susceptibility of these particular regions (corresponded with regional structural alterations) to cause network failures, likely reducing the systemic neuromodulatory effectiveness of GPi-DBS. Accordingly, the ROC and SVM models constructed based on the structural integrity of the regions showing network alterations showed the best power to predict clinical outcome, as shown by the higher AUCs and recall/precision. This further implies that the optimal trade-off between wiring-cost minimization and efficiency of information transfer may play a key role in the outcome of GPi-DBS interventions in dystonia patients.

Our results provide evidence that the balance between short-distance and long-distance connectivity (small-world topology) has direct implications for the GPi-DBS outcome at 3 years. In this regard, computational studies have demonstrated that small-world network architecture requires specific control strategies allowing the enhancement of recovery following system perturbations.<sup>32</sup> Here, we have shown that motor, sensorimotor, and associative regions with impaired microstructure and connectivity (ie, impaired clustering) disturb physiological motor control and counteract normalization of dystonic movements to DBS.<sup>18</sup> Thus, the neuromodulation provided by DBS stimulation exerts specific effects on ongoing brain network activity,<sup>33</sup> and its efficacy depends not only on the local stimulation target, but also relies on the network characteristics.

A limitation of our study could be that electrode localization is an important confounder for DBS outcomes.<sup>34</sup> In our patients, the position of the implant electrodes was projected to the preoperative images and visually checked retrospectively. No clinically relevant shifts of the target that have made reimplantation necessary have been noticed in SOG and MOG. In addition, DYT-1 status has also been reported to be associated with treatment outcome<sup>35</sup>; however, these data were not available for our patients. Previous studies have shown that both dystonia patients with

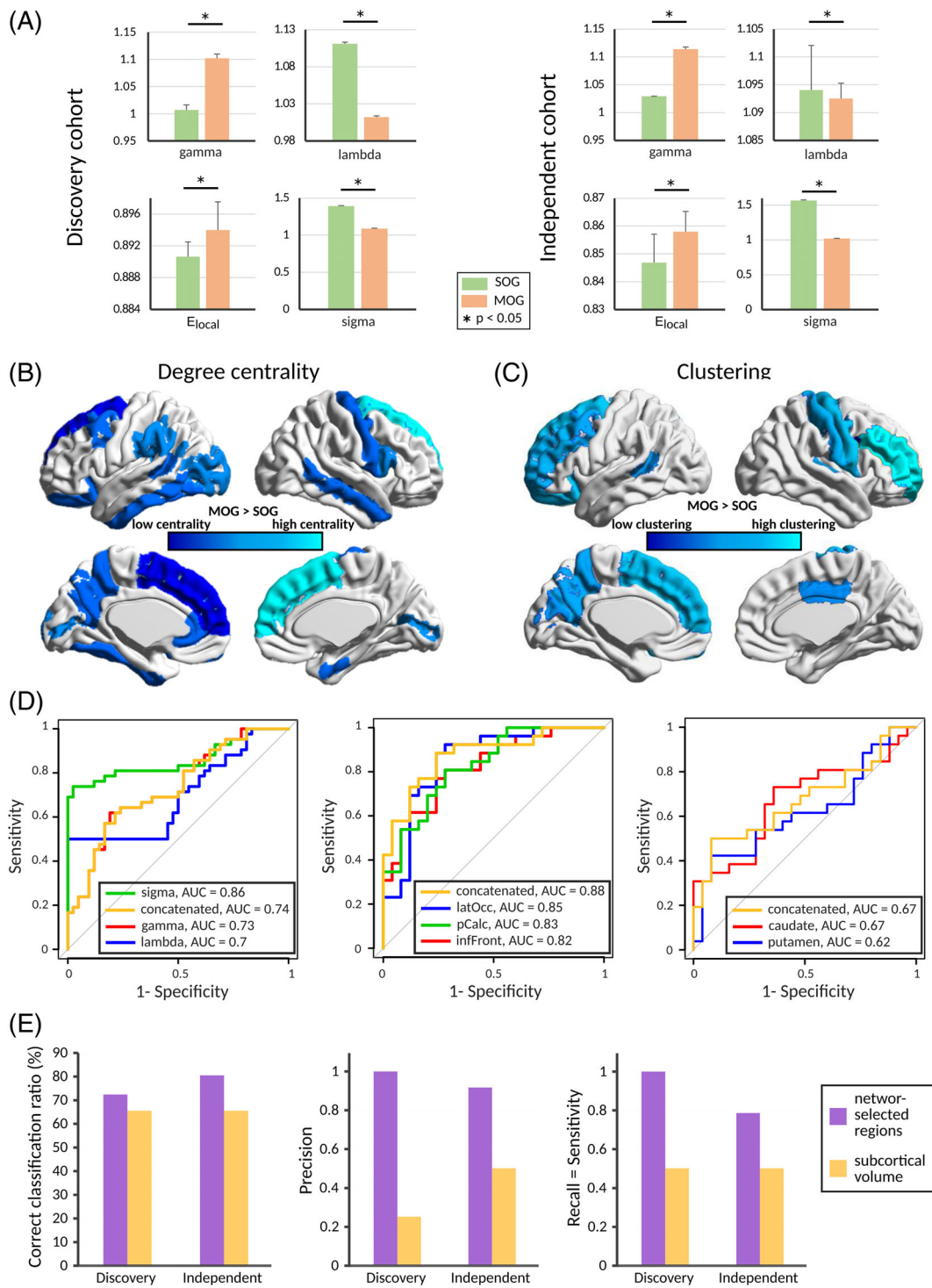


**FIG. 3.** Network and prediction analyses. (A) Between-group differences in network parameters for the discovery (left column), and independent test (right column) cohorts, depicting high clustering and long-range disconnection in MOG (ie, increased gamma and  $E_{local}$  with decreased lambda and sigma). (B, C) Cortical regions showing a higher degree of centrality and clustering coefficient in MOG than in SOG in central and frontoparietal regions. (D) Receiver operating characteristic (ROC) curves with their respective area under the curve (AUC) showing the performance for the network metrics (left), individual regional cortical integrity of regions showing network differences (middle), and subcortical volumes (right) in classifying GPI-DBS outcomes after 3 years. The concatenated variable refers to the accuracy of all the features together. (E) Correct classification ratio (CCR, left), precision (middle), and the recall metrics of the support vector machine for the integrity of the network-selected cortical regions (purple) and the volume of subcortical regions presenting group differences (yellow). latOcc, lateral occipital; pCalc, pericalcarine; infFront, inferior frontal; MOG, moderate-outcome group, SOG: superior-outcome group. [Color figure can be viewed at [wileyonlinelibrary.com](http://wileyonlinelibrary.com)]

DYT-1 and without a known genetic cause showed marked improvement after GPi-DBS.<sup>36</sup> Hence, future studies should control for this in larger populations.

Despite the apparent difference between the groups in mean age, the age distribution of the samples did not differ between the SOG and MOG groups or the independent test cohort and was not associated with any of the study variables. Therefore, age was further included in all the study analyses as a confounder. Hence, the reported differences are unlikely to be driven by aging or sex effects. Related to this, the cohort of patients used in this study did not include symptomatic or secondary dystonia forms and presented a comparable disease history. Other forms of neurological or psychiatric disorders were excluded before inclusion. Therefore, the patient group as a whole represented a relatively homogenous group before surgery in clinical terms. Nevertheless, further studies should be conducted with a focus on more specific disease trajectories and bigger populations of patients.

A further limitation of this study is related to the covariance networks being based on population variances, which do not yield individual metrics. This hampers the possibility of going beyond group-level networks (ie, informing about topological differences between MOG and SOG) and directly performing network-based predictions for the DBS outcomes. Methods for generating individual covariance networks based on single or multiple anatomical features have been proposed.<sup>37-41</sup> However, most of these methods are limited at evaluating grey matter intensity values<sup>41</sup> or need the use of combined and more sophisticated MRI sequences.<sup>40</sup> The latter method further ignores that different anatomical features depict differential nonoverlapping anatomical properties<sup>42</sup> and have specific neurological and genetic underpinnings.<sup>43</sup> Among other well-documented disadvantages,<sup>44</sup> tissue intensity encapsulates combined tissue features, which renders this measure largely redundant and decreases its discriminative power, harshening the detection of some local effects that may be relevant for studying network topology. Hence, determination of individual network metrics remains an open topic.

Overall, our study shows that the individual morphometric integrity profiles in combination with analysis of altered network topology at the group level have a strong potential for better understanding disease trajectories and predicting GPi-DBS outcomes in patients with dystonia. Therefore, the proposed framework can be extended for deciding and assessing the effects of personalized therapeutic approaches and when selecting patients who are likely to benefit from this therapy. ■

**Acknowledgments:** The authors thank Cheryl Ernest and Rosalind Gilchrist for proofreading the manuscript.

## References

- Volkman J, Mueller J, Deuschl G, et al. Pallidal neurostimulation in patients with medication-refractory cervical dystonia: a randomised, sham-controlled trial. *Lancet Neurol* 2014;13(9): 875–884.
- Volkman J, Wolters A, Kupsch A, et al. Pallidal deep brain stimulation in patients with primary generalised or segmental dystonia: 5-year follow-up of a randomised trial. *Lancet Neurol* 2012;11(12): 1029–1038.
- Groppa S, Herzog J, Falk D, Riedel C, Deuschl G, Volkman J. Physiological and anatomical decomposition of subthalamic neurostimulation effects in essential tremor. *Brain* 2014;137(Pt 1): 109–121.
- Koirala N, Fleischer V, Glaser M, et al. Frontal Lobe Connectivity and Network Community Characteristics are Associated with the Outcome of Subthalamic Nucleus Deep Brain Stimulation in Patients with Parkinson's Disease. *Brain Topogr* 2018;31(2):311–321.
- Muthuraman M, Deuschl G, Koirala N, Riedel C, Volkman J, Groppa S. Effects of DBS in parkinsonian patients depend on the structural integrity of frontal cortex. *Sci Rep* 2017;7:43571.
- Hanganu A, Muthuraman M, Chirumamilla VC, et al. Grey Matter Microstructural Integrity Alterations in Blepharospasm Are Partially Reversed by Botulinum Neurotoxin Therapy. *PLoS One* 2016;11(12):e0168652.
- Lehericy S, Tijssen MA, Vidailhet M, Kaji R, Meunier S. The anatomical basis of dystonia: current view using neuroimaging. *Mov Disord* 2013;28(7):944–957.
- Battistella G, Termsarasab P, Ramdhani RA, Fuertinger S, Simonyan K. Isolated Focal Dystonia as a Disorder of Large-Scale Functional Networks. *Cereb Cortex* 2017;27(2):1203–1215.
- Prudente CN, Hess EJ, Jinnah H. Dystonia as a network disorder: what is the role of the cerebellum? *Neuroscience* 2014;260:23–35.
- Quartarone A, Hallett M. Emerging concepts in the physiological basis of dystonia. *Mov Disord* 2013;28(7):958–967.
- Hendrix CM, Vitek JL. Toward a network model of dystonia. *Ann N Y Acad Sci* 2012;1265:46–55.
- Miocinovic S, Miller A, Swann NC, Ostrem JL, Starr PA. Chronic deep brain stimulation normalizes scalp EEG activity in isolated dystonia. *Clin Neurophysiol* 2018;129(2):368–376.
- Neumann WJ, Jha A, Bock A, et al. Cortico-pallidal oscillatory connectivity in patients with dystonia. *Brain* 2015;138(Pt 7): 1894–1906.
- Dec M, Tutaj M, Rudzinska M, et al. Subthalamic nucleus deep brain stimulation after bilateral pallidotomy in the treatment of generalized dystonia. *Parkinsonism Relat Disord* 2014;20(1):131–133.
- Whitmer D, de Solages C, Hill B, Yu H, Henderson JM, Bronte-Stewart H. High frequency deep brain stimulation attenuates subthalamic and cortical rhythms in Parkinson's disease. *Front Hum Neurosci* 2012;6:155.
- Bullmore E, Sporns O. Complex brain networks: graph theoretical analysis of structural and functional systems. *Nat Rev Neurosci* 2009;10(3):186–198.
- Stam CJ. Modern network science of neurological disorders. *Nat Rev Neurosci* 2014;15(10):683–695.
- Bassett DS, Bullmore ET. Small-World Brain Networks Revisited. *Neuroscientist* 2017;23(5):499–516.
- Sporns O, Zwi JD. The small world of the cerebral cortex. *Neuroinformatics* 2004;2(2):145–162.
- Backhausen LL, Herting MM, Buse J, Roessner V, Smolka MN, Vetter NC. Quality Control of Structural MRI Images Applied Using FreeSurfer-A Hands-On Workflow to Rate Motion Artifacts. *Front Neurosci* 2016;10:558.
- Starr PA, Turner RS, Rau G, et al. Microelectrode-guided implantation of deep brain stimulators into the globus pallidus internus for dystonia: techniques, electrode locations, and outcomes. *J Neurosurg* 2006;104(4):488–501.

22. Coubes P, Vayssiere N, El Fertit H, et al. Deep brain stimulation for dystonia. Surgical technique. *Stereotact Funct Neurosurg* 2002;78(3–4):183–191.
23. Ellis TL. Dystonia and the role of deep brain stimulation. *ISRN Surg* 2011;2011:193718.
24. Reese R, Volkmann J. Deep Brain Stimulation for the Dystonias: Evidence, Knowledge Gaps, and Practical Considerations. *Mov Disord Clin Pract* 2017;4(4):486–494.
25. Fischl B. FreeSurfer. *Neuroimage* 2012;62(2):774–781.
26. Desikan RS, Segonne F, Fischl B, et al. An automated labeling system for subdividing the human cerebral cortex on MRI scans into gyral based regions of interest. *Neuroimage* 2006;31(3):968–980.
27. Rubinov M, Sporns O. Complex network measures of brain connectivity: uses and interpretations. *Neuroimage* 2010;52(3):1059–1069.
28. Achard S, Bullmore E. Efficiency and cost of economical brain functional networks. *PLoS Comput Biol* 2007;3(2):e17.
29. Hosseini SM, Hoeft F, Kesler SR. GAT: a graph-theoretical analysis toolbox for analyzing between-group differences in large-scale structural and functional brain networks. *PLoS One* 2012;7(7):e40709.
30. Muthuraman M, Fleischer V, Kolber P, Luessi F, Zipp F, Groppa S. Structural Brain Network Characteristics Can Differentiate CIS from Early RRMS. *Front Neurosci* 2016;10:14.
31. Hoffmann M. The human frontal lobes and frontal network systems: an evolutionary, clinical, and treatment perspective. *ISRN Neurol* 2013;2013:892459.
32. Hubler MJ, Buchman TG. Mathematical estimates of recovery after loss of activity: II. Long-range connectivity facilitates rapid functional recovery. *Crit Care Med* 2008;36(2):489–494.
33. Muldoon SF, Pasqualetti F, Gu S, et al. Stimulation-Based Control of Dynamic Brain Networks. *PLoS Comput Biol* 2016;12(9):e1005076.
34. Pauls KAM, Krauss JK, Kampfer CE, et al. Causes of failure of pallidal deep brain stimulation in cases with pre-operative diagnosis of isolated dystonia. *Parkinsonism Relat Disord* 2017;43:38–48.
35. Bronte-Stewart H, Taira T, Valldeoriola F, et al. Inclusion and exclusion criteria for DBS in dystonia. *Mov Disord* 2011;26(Suppl 1):S5–S16.
36. Park HR, Lee JM, Ehm G, et al. Long-Term Clinical Outcome of Internal Globus Pallidus Deep Brain Stimulation for Dystonia. *PLoS One* 2016;11(1):e0146644.
37. Batalle D, Munoz-Moreno E, Figueras F, Bargallo N, Eixarch E, Gratacos E. Normalization of similarity-based individual brain networks from gray matter MRI and its association with neurodevelopment in infants with intrauterine growth restriction. *Neuroimage* 2013;83:901–911.
38. Kong XZ, Liu ZG, Huang LJ, et al. Mapping Individual Brain Networks Using Statistical Similarity in Regional Morphology from MRI. *PLoS One* 2015;10(11).
39. Li W, Yang C, Shi F, et al. Construction of Individual Morphological Brain Networks with Multiple Morphometric Features. *Front Neuroanat* 2017;11:34.
40. Seidlitz J, Vasa F, Shinn M, et al. Morphometric Similarity Networks Detect Microscale Cortical Organization and Predict Inter-Individual Cognitive Variation. *Neuron* 2018;97(1):231–247.
41. Tijms BM, Series P, Willshaw DJ, Lawrie SM. Similarity-based extraction of individual networks from gray matter MRI scans. *Cereb Cortex* 2012;22(7):1530–1541.
42. Storsve AB, Fjell AM, Tamnes CK, et al. Differential longitudinal changes in cortical thickness, surface area and volume across the adult life span: regions of accelerating and decelerating change. *J Neurosci* 2014;34(25):8488–8498.
43. Winkler AM, Greve DN, Bjuland KJ, et al. Joint Analysis of Cortical Area and Thickness as a Replacement for the Analysis of the Volume of the Cerebral Cortex. *Cereb Cortex* 2018;28(2):738–749.
44. Ashburner J. Computational anatomy with the SPM software. *Magn Reson Imaging* 2009;27(8):1163–1174.

## Supporting Data

Additional Supporting Information may be found in the online version of this article at the publisher's web-site.